On the Multivariate Regression Modeling for Performance Prediction of Dew-point Evaporative Desalination System

Muhammad Imran Haider
Department of Agricultural Engineering, Bahauddin Zakariya University

Hafiz Muhammad Asfahan
Department of Agricultural Engineering, Bahauddin Zakariya University

Sultan, Muhammad
Department of Agricultural Engineering, Bahauddin Zakariya University

KYUSHU UNIVERSITY

On the Multivariate Regression Modeling for Performance Prediction of Dew-point Evaporative Desalination System

Muhammad Imran Haider[1,†], Hafiz Muhammad Asfahan[1,†], Muhammad Sultan[1,*]

[1]Department of Agricultural Engineering, Bahauddin Zakariya University, Multan 60800, Pakistan

*Corresponding author email: muhammadsultan@bzu.edu.pk

Abstract: *Desalination is a standalone solution to extract the water beyond the natural water hydrological cycle aiming for extracting freshwater that mitigates the water supply-demand gap. The present study focused to develop a multivariate regression model (MRM) for performance prediction of the dewpoint evaporative desalination (DPD) system in accordance with the climatic conditions of Pakistan. For doing so, experimental results of the DPD system were collected from the literature, and developed MRM models considering both two-stage and three-stage DPD systems. The developed models were then used to predict specific energy consumption (SEC) and daily water production (DWP). For the two-stage configuration, root means square error (RMSE) was found at 0.088 and 0.004 for SEC and DWP, whereas, in the three-stage configuration, RMSE was observed at 0.074 and 0.006, respectively. In Karachi and Gwadar climatic scenario, the DPD system have potential to produce an average DWP of 0.7237 m³/day/m³/sec. According to Köppen–Geiger climate classification, arid (Bwk), desert climate (Bwh), semi-arid (BSh), and humid subtropical region (Cwa) are the promising localities to drive and DPD system.*

Keywords: Dew point evaporative desalination; Köppen–Geiger climate; Multivariate regression modeling; Pakistan;

1. INTRODUCTION

Since the 1980s, the global water consumption has been growing at a 1% annual rate [1, 2]. There are already around one-fifth of the world's people who live under the water availability limit of 500 m³ per capita per year [3]. Pakistan will be a water-scarce nation by 2025 if present trends continue and water supply drops to roughly 800 m³ per person and demand rises by 6 percent [3]. By 2050, an estimated five billion people would be affected by water shortages as a result of population growth, according to the United Nations [4]. Alternative freshwater reserves are principally required to accommodate the global thirst.

Desalination is a feasible solution to the issue of water scarcity since it removes salts from salt water. (a) thermal-driven like vapor compression (VC), multi-stage flashing (MSF) [5, 6], multi-effect distillation (MED) [7], membrane distillation (MD) [8], humidification-dehumidification desalination (HDD) [9], solar still, adsorption desalinization (AD) [10–12] and (b) mechanical-driven like electrodialysis (ED), and reverse osmosis [13]. Scaling, the precipitation of inorganic salts from solution onto a surface, is a common problem in all of these desalination procedures. The buildup of inorganic foulants in heat exchangers and evaporators in thermal desalination plants reduces heat transmission and increases the risk of clogging and corrosion. The establishment of scale therefore has a substantial impact on desalination process performance and often results in maintenance outages. It's incredibly efficient to compress vapor mechanically. However, compared to thermal vapor compression, it has greater operating and maintenance expenses and necessitates the use of a large external heating source. Plants using MSF have scaling concerns. The heated brine is flash distilled at a lower temperature and pressure in this process. The feed saltwater is heated continually as it passes through the various stages, and the heat exchange mechanisms also allow condensation to occur, which is used to recover fresh water for reuse [5, 14]. Scaling in RO processes decreases membrane permeability, raises energy consumption, and degrades membrane durability. With the inclusion of pretreatment operations, as well as frequent cleaning and maintenance, RO's operating costs might rise significantly [11, 15, 16].

Scaling concerns during spray evaporation make it incompatible with higher temperature heat sources. Because of the intricacy and huge number of components needed, it is also difficult to scale down to tiny scales. New, low-energy desalination methods must be developed to maintain reasonable water pricing in locations with limited access to potable water. Dew point desalination based on indirect evaporative cooling is one of the most promising techniques that might become a new source of clean water with minimum energy usage. It is crucial for regional prosperity as well as economic and political stability to have access to high-quality drinking water.

An increase in the temperature from 30 °C to 60 °C resulted in an increase in total water production by 47% in the system. Similarly, an increase in the humidity by reducing the vapor volume can also improve the water production rate. It was demonstrated that the total water production is increased by 58% when the vapor volume in the evaporation chamber is reduced from 600 cm³ to 400 cm³ [17]. A maximum increase in productivity of about 98% was achieved for stepped solar stills when fins, sponge and pebbles were used [18]. In solar-driven membrane, it was found that a system with a solar absorbing area of 1.6 m² integrated with ~0.2 m² of membranes can produce ~4 L of drinkable water and ~4.5 kWh of heat energy (at 45 °C) per day (with an average daily solar exposure of 4 kWh/m²) [19]. Solar distillation presents a promising alternative for saline water desalination that can partially support humanity's needs for fresh water with free energy, simple technology and a clean environment. Producing fresh water by solar distillation can support community living activities, particularly in rural areas, when weather conditions are suitable and demand is not too great, i.e., less than 200 m³/d [20].

Dew point desalination technology is energy efficient method. By the graphical data of specific energy consumption (kWh/m^3) (SEC) daily water production (m^3/day/m^3/sec) (DWP) Inlet air temperature, (ºC) and Inlet humidity ratio, (g/kg).by this data perform multivariate regression analysis and developed regression models and general equations. The developed models were used to predict the performance of the dewpoint evaporative desalination (DPD) system in accordance with climatic conditions of Pakistan. In addition, the analysis extends to the Köppen–Geiger to identify the localities that could be favorable for installation of DPD system worldwide.

2. WORKING PRINCIPLE OF DEW-POINT EVAPORATIVE SYSTEM

Fig. 1. depicts the DPD system's functioning schematic of the DPD system. In stage-1 (inlet1), the air is cooled without a significant rise in its moisture content (inlet1-outlet1). cooling air (outlet1) is split into two halves. Output 1 becomes input 2 in the first step and output 1 becomes input 3 in the second stage. In the first working step, salt water is sprayed on the inner plates. evaporation of water from the plate surface into the working air that travels via the working channel (inlet2-outlet2) causes sensible cooling Because the salt water's mineral compounds don't evaporate, the stream of water is what flushes them out of the exchanger. Stage 2 is supplied with humidified working air that has been carried from output 2 (the dew point cooler) in stage 1. To begin with, at stage 2 (inlet4), the product air has a higher moisture content than in stage 1 (inlet1) (inlet1). Stage 2's wet product air is inadvertently mixed with the working air in the next channel (inlet3). Working air in stage-1 (inlet1-outlet1) is much cooler than the product air in the neighboring channel Because of pre-cooling in stage-1 (inlet4). The addition of water evaporation was thus chosen as a method for creating sensible cooling. At a lower temperature on the plate that divides the work and product channels, water vapor is more likely to condense on the plates of the product channel in stage 2 under these conditions. It is possible to collect this condensate, which has a very low salt content, and use it in water treatment.
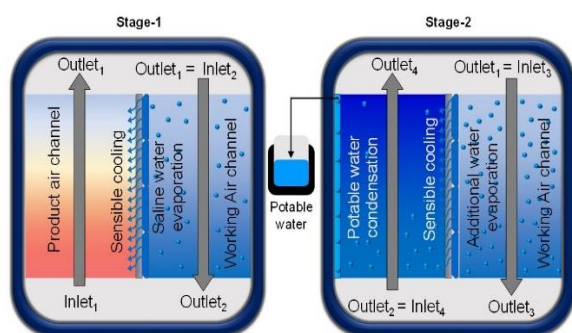

Fig. 1. Working schematic of dewpoint evaporative desalination system.

Fig. 2 (a) and Fig. 2 (b) shows the psychrometric presentation stage-1 and stage-2 of the DPD system, respectively. During stage-1 as shown in Fig.2. (a) the ambient air is cool down until the dewpoint temperature

achieves and after that humidification process executes at 100% relative humidity line. Delivered airflow enters the product channels after being delivered to the first stage of DPD (1i in Fig. 2a). Due to the sensible heat transfer to the nearby working channels, air flowing through the product channels is chilled (1i-1o). Utilizing dew point cooling technology, it is possible to chill product channels (1o) almost to their dew point temperature (t1iDP), without increasing the moisture content of the air. The cooled air is split into two pieces when it exits the product channels. The first portion (1o = 2i) is routed to the dew point cooler's operating channels, while the second portion (1o = 3i) is employed in the second stage of DPD. In the first step (2i), a portion of the air enters working channels where it comes into contact with salt water that has been distributed out on the plate surface. Saltwater absorbs heat from both the working air and the air flowing in the neighboring product channel. This heat transfer causes the water to evaporate into the working air, humidifying it and raising its temperature (2i-2o). Because seawater minerals do not evaporate, the desalination process is successful. Air that leaves the working channel (2o) is saturated and has a significantly higher moisture content than the air that enters the channel (2i). After the first stage, the second stage (1o = 3i) delivers airflow from the product channels to the working channels, and the second stage (2o = 4i) delivers airflow from the working channels to the product channels. Water begins to condense on the plate surface of the product channels because the air entering the working channels in the second stage (3i) is warmer than the air entering the dew point channels (4i), which results in the dehumidification of the product air (4i–4o). The surrounding working channels receive any sensible or latent heat that is emitted with the condensing of water in the product channel. The inner plates in the working channel are also covered in saltwater that evaporates to the working airflow, so its moisture content and temperature raises ($3i = 3o$). Once the supplied air will completely saturate the process air than dehumidified in order to acquire freshwater as described in Fig. 2 (b)

3. METHODOLOGY

To investigate the performance of the DPD system in accordance with the climatic conditions, the experimental data are taken from the cited literature [21] and perform the regression analysis using MS excel. The effectiveness of dewpoint evaporative system is 1.2 [21–24]. Four multivariate regression models are developed: (i) two-stage DPD system for predicting the SEC, (ii) two-stage DPD system for predicting the DWP, (iii) three-stage DPD system for predicting the SEC, and (iv) three-stage DPD system for predicting the DWP. All the developed models are the function of the inlet temperature and inlet humidity ratio which allows to consider the influential psychrometric variables.

4. VALIDATION OF THE DEVELOPED MODEL

Fig. 3 (a) and Fig.3 (b) show the Validation of the developed MRM for two-stage DWP and SEC having a root mean square error (RMSE) of 0.0040 and 0.0885, respectively. Fig. 4 (a) and Fig. 4 (b) depict the

Validation of three-stage DWP and SEC having RMSE of 0.0057 and 0.0743, respectively. It has been observed that the RMSE is in the acceptable range and the developed model can be used effectively for anticipating the DWP and SEC following the climatic conditions of Pakistan. The DWP changes linearly so it could be stated that the increase of temperature by two Celsius degrees causes the DWP to increase by 0.055 (m^3/day/m^3/sec) for the 2-stage DPD system and by 0.089 (m^3/day/m^3/sec) for the 3-stage DPD system. The SEC changes from a maximum value at t1i = 24 °C, 1.48 (kWh/m^3) for the 2-stage DPD system and 1.40 (kWh/m^3) for the 3-stage DPD system) to the minimum value at t1i = 34 °C (0.54 (kWh/m^3) for the 2-stage DPD system and 0.46 (kWh/m^3) for the 3-stage DPD system). In all analyzed cases, the 3-stage DPD system is more beneficial either in terms of lower SEC and higher DWP than the 2-stage DPD system. The DWP depending on humidity ratio x1i also changes linearly so it could be stated that the increase of humidity ratio by 2(g/kg) causes the DWP to increase by 0.052 (m3/day/m3/sec) for the 2-stage DPD system and by 0.084 (m3/day/m3/sec) for the 3-stage DPD system. The SEC changes from minimum value at x1i = 8(g/kg), 0.60 (kWh/m^3) for the 2-stage DPD system and 0.30 (kWh/m^3) for the 3-stage DPD system) to the maximum value at x1i = 18 (g/kg),1.44 (kWh/m^3) for the 2- stage DPD system and 1.36 (kWh/m^3) for the 3-stage DPD system). In all analyzed cases, the 3-stage DPD system is more beneficial either in terms of lower SEC or higher DWP than the 2-stage DPD system.
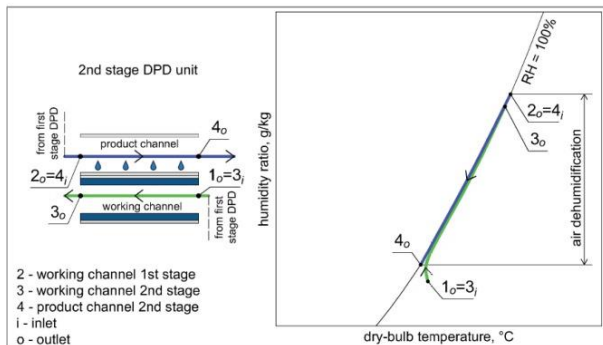
(a)
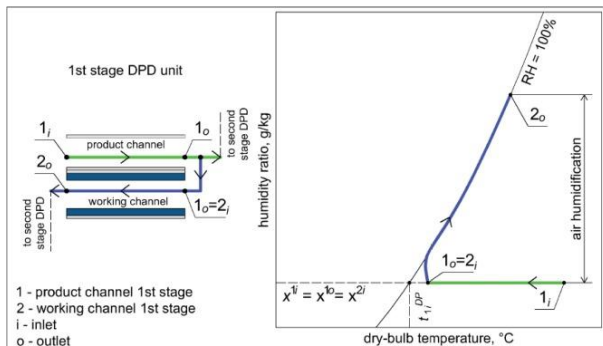
(b)

Fig. 2. Dewpoint evaporative desalination psychometric process representation reproduce here from [21].
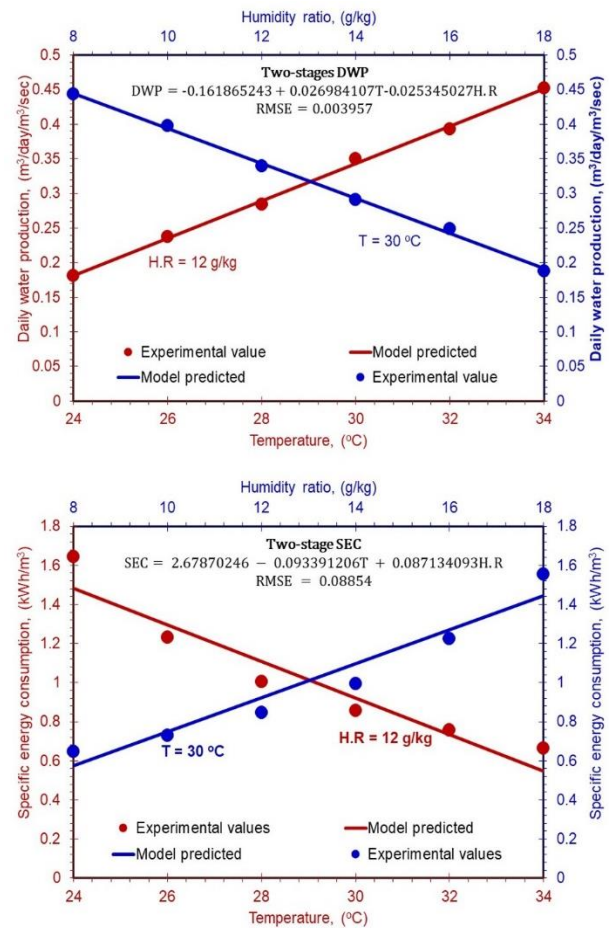.

Fig. 3. Validation of developed two-stage DWP and SEC models.

5. RESULTS AND DISCUSSION

Fig. 3. Shows the Validation of developed two-stage DWP and SEC models. First graph is the combination of Temperature, (24-34, °C), Humidity ratio, (8-18 g/kg), and Daily water production DWP, (0-1.8, m3/day/m3/sec). The maximum and minimum values of the experimental value are 0.4523 and 0.1813 against temperatures of 34 and 24, (°C) at a constant Humidity ratio, (12, g/kg). And the maximum and minimum value models predicted are 0.4514 and 0.1816 against temperatures of 34 and 24, (°C) at a constant Humidity ratio, (12, g/kg) respectively. Similarly, the maximum and minimum values of the experimental value are 0.4441 and 0.1883 against Humidity ratios of 8 and 18, (g/kg) at a constant temperature, (30, °C). And values of the model predicted are 0.4448 and 0.1914 against humidity ratios of 8 and 18, (g/kg) at a constant temperature, (30, °C) respectively. The second graph is the combination of Temperature, (24-34, °C), Humidity ratio, (8-18 g/kg), and Specific energy consumption, (kWh/m3). The maximum and minimum values of the experimental values are 1.6433 and 0.6635 against temperatures of 24 and 34, (°C) at a constant Humidity ratio, (12, g/kg). And values of the model predicted are 1.4829,0.5490 against temperatures of 24 and 34, (°C) at constant Humidity ratio, (12, g/kg) respectively. Similarly, the maximum and minimum values of the experimental value are 1.5534 and 0.6466 against Humidity ratios of 18 and 8, (g/kg) at a constant

temperature, (30, °C). And values of the model predicted are 1.4453 and 0.5740 against humidity ratios of 18 and 8, (g/kg) at a constant temperature, (30, °C) respectively.
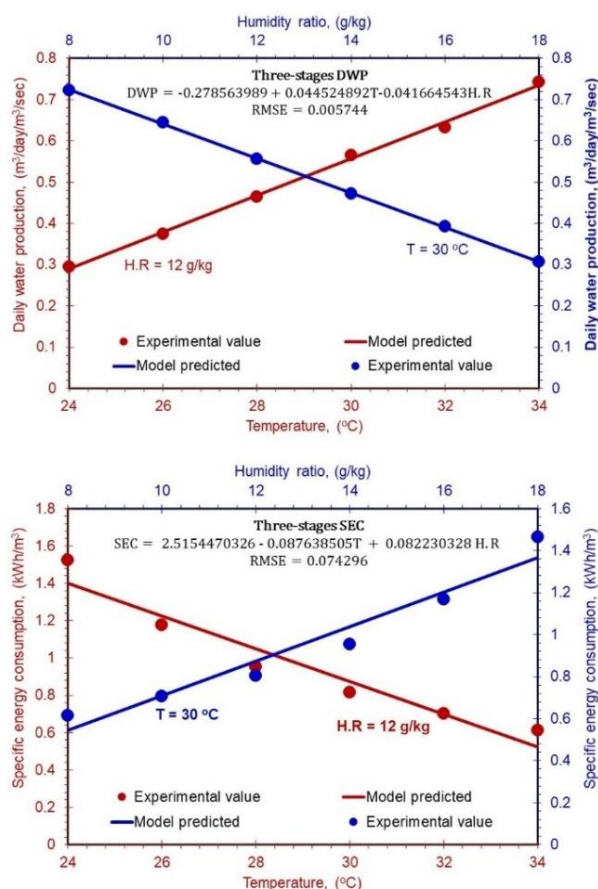

Fig. 4. Validation of developed three-stage DWP and SEC models.

Fig. 4. Shows the Validation of developed three-stage DWP and SEC models. The first graph is the combination of Temperature, (24-34, °C), Humidity ratio, (8-18 g/kg), and Daily water production DWP, (0-1.8, m3/day/m3/sec). The maximum and minimum values of the experimental value are 0.7428 and 0.2953 against temperatures of 34 and 24, (°C) at a constant Humidity ratio, (12, g/kg). And the maximum and minimum values of models predicted are 0.7353 and 0.29005 against temperatures of 34 and 24, (°C) at a constant Humidity ratio, (12, g/kg) respectively. Similarly, the maximum and minimum values of the experimental value are 0.7232 and 0.3069 against Humidity ratios of 8 and 18, (g/kg) at a constant temperature, (30, °C). And values of the model predicted are 0.7238 and 0.3072 against humidity ratios 8 and 18, (g/kg) at a constant temperature, (30, °C) respectively. The second graph is the combination of Temperature, (24-34, °C), Humidity ratio, (8-18, g/kg), and Specific energy consumption, (kWh/m3). The maximum and minimum values of the experimental value are 1.5247 and 0.6146 against temperatures of 24 and 34, (°C). And values of the model predicted are 1.3988 and 0.5225 against temperatures of 24 and 34, (°C) at a constant Humidity ratio, (12, g/kg) respectively. Similarly, the maximum and minimum values of the experimental

value are 1.4635 and 0.6139 against Humidity ratios of 18 and 8, (g/kg) at a constant temperature, (30, °C). And values of the model predicted are 1.3664 and 0.5441 against humidity ratios of 18 and 8, (g/kg) at a constant temperature, (30, °C) respectively.

Fig. 5. Show the prediction value of DWP for two-stage and three-stage configurations for the climatic conditions of Karachi and Gwadar, (Pakistan). In this graph, the maximum value of DWP for two-stage are 0.7319, (m3/day/m3/sec) against temperature, (33.14, °C) and humidity ratio, (15.74, g/kg) and minimum value are 0.2846, (m3/day/m3/sec) against temperature, (16.55, °C) and humidity ratio, (3.5612, g/kg). And the maximum value of DWP for the three-stage are 1.1963, (m3/day/m3/sec), against temperature, (33.14, °C) and humidity ratio, (15.74, g/kg) and the minimum value are 0.4581, (m3/day/m3/sec) against temperature, (16.55, °C) and humidity ratio, (3.5612, kg/kg). The above graph also defines the prediction value for the same configuration for the climatic condition of Gwadar, here the maximum, and minimum values for two-stage and three-stage are 0.6980, (m3/day/m3/sec) against temperature, (31.89, °C) and humidity ratio, (23.3336, g/kg) and 0.2463, (m3/day/m3/sec) against temperature, (15.13, °C) and humidity ratio, (3.2503, g/kg), respectively. And the maximum and minimum values for three-stage of daily water production are 1.1403, (m3/day/m3/sec) against temperature, (31.89, °C) and humidity ratio, (23.3336, g/kg) and 0.3949, (m3/day/m3/sec) against temperature, (15.13, °C) and humidity ratio, (3.2503, g/kg) respectively.
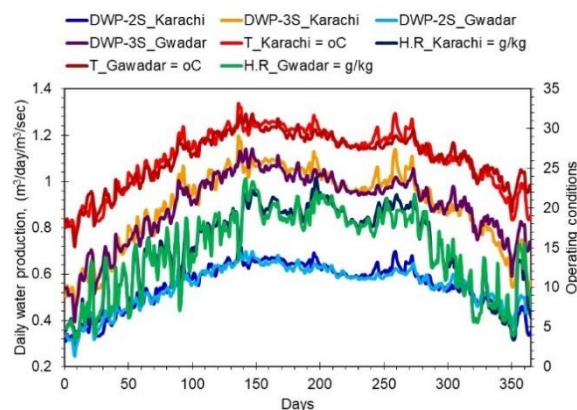

Fig. 5. Prediction of DWP from two-stage and three-stage configuration for the climatic conditions of Karachi and Gwadar.

Fig. 6. Show the prediction value of SEC for two-stage and three-stage configurations for the climatic conditions of Karachi and Gwadar, (Pakistan). In this graph, the maximum and minimum values of SEC for two-stage are 1.0653 and -0.3876, (kWh/m3) respectively.
And the maximum and minimum values of SEC for the three-stage are 1.1333 and -0.4149, (kWh/m3) respectively. The above graph also defines the prediction value for the same configuration for the climatic condition of Gwadar, here the maximum, and minimum values of two-stage and three-stage are 1.1897 and -0.2774, (kWh/m3) and 1.2649 and -0.2975, (kWh/m3) respectively. This figure's center contains a dead zone,

indicating that no water production was discovered there. In terms of cooling potential or SEC, dead zone of about 100 days were observed which reflect the system is not functional for cooling applications during that period either from two-stage and three-stage configuration.
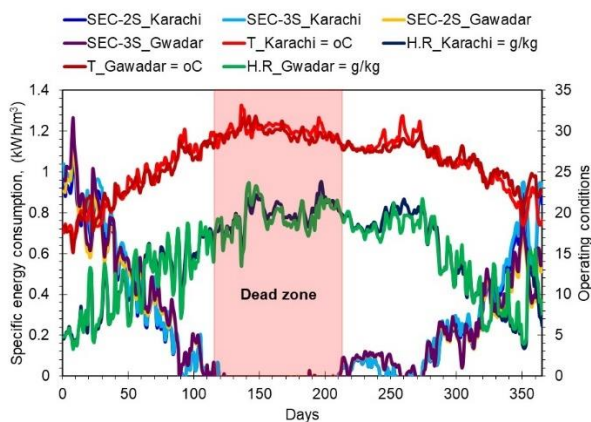

Fig. 6. Prediction of SEC from two-stage and three-stage configuration for the climatic conditions of Karachi and Gwadar.

Fig. 7. shows the performance prediction of the SEC two-stage and DWP two-stage dewpoint evaporation system following Köppen–Geiger climate classification [25]. In this graph, the value of Dsc for the SEC two-stage is 1.6325, (kWh/m3) against temperature, (17.3, ℃) and humidity ratio, (7.7, g/kg) and the value of Bwk is -0.4124, (kWh/m3) against temperature, (38.1, ℃) and humidity ratio, (5, k/kg). The potential of Dsc is higher than Bwk which shows Dsc has high energy consumption. The daily water production for two-stage for Bwk are 0.7395, (m3/day/m3/sec) against temperature, (38.1, ℃) and humidity ratio, (5, k/kg) and the value of Dsc are 0.1098, (m3/day/m3/sec) against temperature, (17.3, ℃) and humidity ratio, (7.7, k/kg). The potential of Bwk is higher than Dsc which shows high water production.
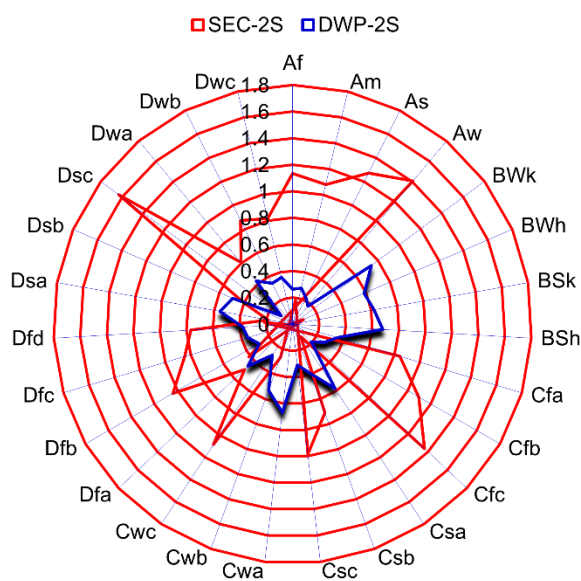

Fig. 7. Performance prediction of the two-stage dewpoint evaporation system in accordance with Köppen–Geiger climate classification.

Fig. 8. shows the performance prediction of the SEC three-stage and DWP three-stage dewpoint evaporation system in accordance with Köppen–Geiger climate classification [25]. In this graph, the Dsc value for the SEC three-stage is 1.7339, (kWh/m3) against temperature, (17.3, ℃) and humidity ratio, (7.7, k/kg) and Bwk value for the SEC three-stage are -0.4438, (kWh/m3) against temperature, (38.1, ℃). The potential of Dsc is higher than Bwk which shows the high energy consumption. And daily water production for three-stage is 1.2035 and 0.1709, (m3/day/m3/sec) for Bwk against temperature, (38.1, ℃) and humidity ratio, (5, k/kg) and 0.1709, (m3/day/m3/sec) for Dsc, against temperature, (17.3, ℃) and humidity ratio, (7.7, k/kg). The potential of Bwk is higher than Dsc which shows high water production.
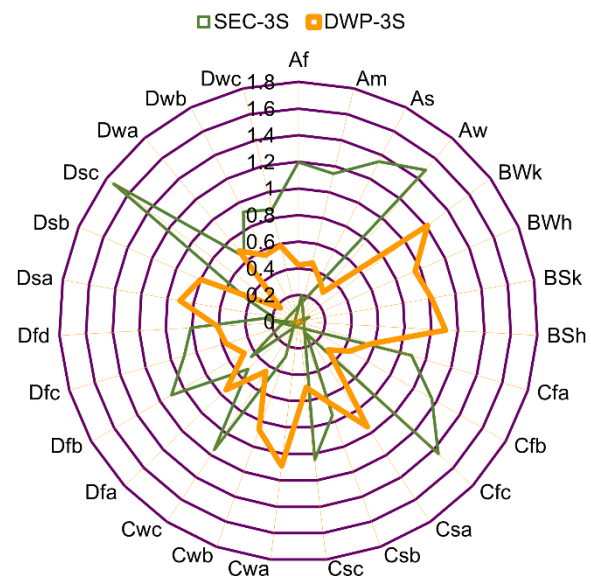

Fig. 8. Performance prediction of the three-stage dewpoint evaporation system in accordance with Köppen–Geiger climate classification.

6. CONCLUSION

The study focused to develop a multivariate regression model (MRM) having independent variables (i.e., temperature and humidity ratio) and dependent variables (i.e., water production rate (WPR) and specific energy consumption (SEC) for predicating the performance of the dewpoint evaporative desalination (DPD) system in accordance with the climatic conditions of Pakistan. The developed models were evaluated based on the statical error determination approach termed as root means square error (RMSE). The developed four models capable to predict the performance indicators of the DPD system having RMSE in acceptable range.

It has been analyzed that, Pakistan is favorable place for producing the freshwater from the studied low-cost, energy-efficient system. Karachi and Gwadar are the most promising localities for the DPD system having DWP capacity of 0.7237, (m3/day/m3/sec). However, in terms of cooling potential or SEC, dead zone of about 100 days were observed which reflect the system is not functional for cooling applications during that period either from two-stage and three-stage configuration. It

has been concluded that the DPD system is even more attractive and appealing for the regions of arid (Bwk), desert climate (Bwh), semi-arid (BSh) and humid subtropical region (Cwa) classified based on the Köppen–Geiger climate.

Acknowledgements

Conflict of interest

The authors declare no conflict of interest.

7. REFERENCES

[1] Ali ES, Muhammad Asfahan H, Sultan M, et al. A novel ejectors integration with two-stages adsorption desalination: Away to scavenge the ambient energy. *Sustain Energy Technol Assessments* 2021; 48: 101658.

[2] UNESCO, UN-Water 2020. *The United Nations World Water Development Report 2020: WATER AND CLIMATE CHANGE*. Paris, 2020.

[3] Gilbert F. Houngbo, Azoulay A. *The United Nations World Water Development Report 2018: NATURE-BASED SOLUTIONS FOR WATER*. 2018.

[4] Connor R, Koncagül E. *The United Nations World Water Development Report 2014: WATER AND ENERGY*. 2014. Epub ahead of print 2014. DOI: 10.46632/rmc/1.

[5] Hashim A, Hajjaj M. Impact of desalination plants fluid effluents on the integrity of seawater, with the Arabian Gulf in perspective. *Desalination*. Epub ahead of print 2005.

[6] El-Dessouky HT, Ettouney HM, Mandani F. Performance of parallel feed multiple effect evaporation system for seawater desalination. *Appl Therm Eng*. Epub ahead of print 2000. DOI: 10.1016/S1359-4311(99)00098-8.

[7] Al-Mutaz IS, Wazeer I. Comparative performance evaluation of conventional multi-effect evaporation desalination processes. *Appl Therm Eng* 2014; 73: 1194–1203.

[8] Zapata-Sierra A, Cascajares M, Alcayde A, et al. Worldwide research trends on desalination. *Desalination* 2022; 519: 115305.

[9] Rahimi-Ahar Z, Hatamipour MS, Ahar LR. Air Humidification-Dehumidification Process for Desalination: A review. *Progress in Energy and Combustion Science* 2020; 80: 100850.

[10] Elsayed E, AL-Dadah R, Mahmoud S, et al. Experimental testing of aluminium fumarate MOF for adsorption desalination. *Desalination* 2020; 475: 114170.

[11] Riaz N, Asfahan HM, Sultan M. Investigation of metal organic frameworks based water desalination and cooling systems. In: *International Conference on Energy, Water and Environment (ICEWE-2021)*. Lahore, Pakistan, 2021, pp. 239–241.

[12] Riaz N, Sultan M, Miyazaki T, et al. A review of recent advances in adsorption desalination technologies. *Int Commun Heat Mass Transf* 2021; 128: 105594.

[13] Sadri S, Khoshkhoo RH, Ameri M. Optimum exergoeconomic modeling of novel hybrid desalination system (MEDAD+RO). *Energy* 2018; 149: 74–83.

[14] Asfahan H, Riaz N, Sultan APM. *Investigating desalination systems working on dew-point evaporation, standalone adsorption and adsorption-ejector methods*. 2021.

[15] El-Dessouky H, Shaban HI, Al-Ramadan H. Steady-state analysis of multi-stage flash desalination process. *Desalination*. Epub ahead of print 1995.

[16] Fritzmann C, Löwenberg J, Wintgens T, et al. State-of-the-art of reverse osmosis desalination. *Desalination*. Epub ahead of print 2007.

[17] Al-madhhachi H, Min G. Key factors a ff ecting the water production in a thermoelectric distillation system. *Energy Convers Manag* 2018; 165: 459–464.

[18] El-sebaii AA, El-bialy E. Advanced designs of solar desalination systems : A review. *Renew Sustain Energy Rev* 2015; 49: 1198–1212.

[19] Li Q, Beier L, Tan J, et al. An integrated , solar-driven membrane distillation system for water purification and energy generation. *Appl Energy* 2019; 237: 534–548.

[20] Fath HES. Solar distillation : a promising alternative for water provision with free energy , simple technology and a clean environment. 116.

[21] Pandelidis D, Cichoń A, Pacak A, et al. Water desalination through the dewpoint evaporative system. *Energy Convers Manag*; 229. Epub ahead of print 2021.

[22] Shabir F, Sultan M, Miyazaki T, et al. Recent updates on the adsorption capacities of adsorbent-adsorbate pairs for heat transformation applications. *Renew Sustain Energy Rev* 2020; 119: 109630.

[23] Noor S, Ashraf H, Hussain G, et al. Spatiotemporal investigation of evaporative cooling options for greenhouse air-conditioning application in Pakistan. *Fresenius Environ Bull*; 21.

[24] Asfahan HM, Sajjad U, Sultan M, et al. Artificial intelligence for the prediction of the thermal performance of evaporative cooling systems. *Energies* 2021; 14: 3946.

[25] Wikipedia. Köppen climate classification - Wikipedia, https://en.wikipedia.org/wiki/Köppen_climate_classification (2021).